Internal Structure of Layer-by-Layer Adsorbed Polyelectrolyte Films: A Neutron and X-ray Reflectivity Study

Johannes Schmitt,[†] Torsten Grünewald,[†] Gero Decher,[†] Peter S. Pershan,[‡,§] Kristian Kjaer,[‡] and Mathias Lösche*,[†]

Institute of Physical Chemistry, Johannes-Gutenberg-Universität Mainz, D-55099 Mainz, Germany, and Physics Department, Risø National Laboratory, DK-4000 Roskilde, Denmark

Received July 8, 1993; Revised Manuscript Received September 1, 1993®

ABSTRACT: The internal structure of ultrathin polymer films physisorbed to surface-modified Si wafers by electrostatic deposition of polyelectrolytes from aqueous solutions has been investigated by measuring the X-ray and neutron reflectivity from partially deuterated samples. For the first time it has been demonstrated that the preparation procedure, which involves repeated dipping of the substrate into solutions of polycations and polyanions in an alternating sequence, leads to the deposition of continuous molecular layers that form a polymer film with a well-defined supramolecular structure. Thus, the structure of a polymer film deposited from solutions with high ionic strength (2 M NaCl) and comprising 48 molecular strata, which were organized in a superlattice of 5 perprotonated layers and 1 perdeuterated layer in 8 repeat units, has been resolved in full detail: the overall layer thickness was found to be 1205 ± 20 Å, the layers deposited close to the substrate had a thickness significantly smaller than their equilibrium thickness far from the substrate, and the equilibrium thickness of an individual polycation layer was ~20 Å and that of the polyanion layer ~35 Å. The surface roughnesses at the substrate/film and the film/air interface were significantly different, ~4 and ~13 Å, respectively, but even the larger number for the film/air interface shows that continuous and molecularly smooth layers are formed. The interdigitation between neighboring polymer layers was estimated to be ~12 Å; the water content of the film has been determined, and the concentration of counterions deposited with the polyelectrolyte has been estimated.

Introduction

Molecular polymer films fall in a category of novel materials where the macroscopic properties can be custom-tailored by the control of the microscopic structure on the level of both the molecular structure and the organization of the consitutent molecules. Hence, self-organization principles play an important role in determining material properties. Recently, Decher and co-workers have introduced an innovative strategy to prepare ultrathin polymer films,[1-3] which are well-organized on the molecular level: polyelectrolytes are physisorbed from solution to charged interfaces via electrostatic interaction. They have been shown to deposit as molecularly thin films and to lead to a reversal of the net charge at the interface upon deposition. This, in turn, opens the possibility for the deposition of a polyelectrolyte film of the opposite charge in a second physisorption step and thus for the sequential buildup of layer-by-layer deposited polyanion/polycation multilayer films.

Evidence for the layer structure was derived from monitoring bulk properties, the sequential increase of the UV-vis absorption, or the total film thickness, using low-angle X-ray reflectivity,[2] but the internal structure of such systems remained largely inaccessible[4] due to the lack of contrast in electron densities of the individual charge-deposited layers. For poly(styrenesulfonate), adsorbed as single layers to positively charged, molecularly smooth interfaces, a layer thickness in the regime of 15-25 Å has been reported.[5,6] In this work, we have employed neutron reflectivity measurements on samples incorporating superstructures of protonated and deuterated polyelectrolytes to assess directly individual layer thicknesses and the roughness of internal interfaces as well as to estimate the material densities and water and salt contents of the deposited films. These measurements were complemented with X-ray reflectivity measurements to determine precisely the overall sample thickness and density and to characterize the bare substrates.

Reflectivity Measurements

Measurements of the specular X-ray and neutron reflectivity have been extensively utilized to characterize the structures of planar surfaces, both fluid and solid, on the molecular length scale.[7-11] In particular, these methods have been shown to be extremely useful for the characterization of thin polymer films.[10,12,13] The physics underlying specular reflectivity techniques are extensively discussed in the literature cited above. Here, we just recall that the specularly reflected intensity of a neutron or X-ray beam contains information on the scattering length density (SD) profile perpendicular to the surface (surface normal: $\hat{z}$), due to the interference of waves reflected at external or internal interfaces of the film. In the kinematic approximation, the reflectivity R is connected with $\rho(z)$ via[7,14,15]

$$\frac{R(Q_z)}{R_F(Q_z)} = \frac{1}{\rho_0^2}\left|\int_{\text{interface}} \frac{d\rho(z)}{dz} \exp(iQ_z z)\, dz\right|^2 \qquad (1)$$

where Q_z is the momentum transfer, R_F is the Fresnel reflectivity of the bare planar substrate, and ρ_0 is the substrate's SD. This approximation holds in the range $Q_z \gtrsim 5Q_c$, where Q_c is the critical wave vector for total external reflection. Due to the phase problem, $\rho(z)$ cannot in general be directly reconstructed from the reflectivity data, although a model-independent reconstruction technique has been recently reported.[5] The scattering length density

* To whom correspondence should be addressed.
† Institute of Physical Chemistry, Johannes-Gutenberg-Universität Mainz.
‡ Physics Department, Risø National Laboratory.
§ Permanent address: Physics Department and Division of Applied Science, Harvard University, Cambridge, MA 02138.
® Abstract published in *Advance ACS Abstracts*, November 1, 1993.

0024-9297/93/2226-7058$04.00/0

profile is thus usually obtained from model refinement of the interface structure, e.g., by using least-squares methods. The sequential deposition of alternately charged polyelectrolytes on the substrate that is used for sample preparation suggests that one use as a reasonable guess for a trial structure a model where $\rho(z)$ is composed of a number of polymer layers with interfaces at the locations z_i:

$$\rho(z) = \sum_{i=0}^{n} [(\rho_{i+1} - \rho_i)/2](1 - \mathrm{erf}[(z - z_i)/2^{1/2}\sigma_i]) \quad (2)$$

Here, erf[z] is the normalized error function, $\delta(z)$ is the normalized delta function, and $\rho_{n+1} = 0$ (in air). The substrate/film and the film/air interfaces are located at $z = z_0$ and z_n, respectively. The SD profile can then be interpreted in terms of the thicknesses, $d_i = (z_{i+1} - z_i)$, of individual polymer layers, their material density (connected with the SDs, ρ_i, via the scattering lengths), and the roughness of the interfaces, σ_i, which, for internal interfaces, may be conceived as the roughness due to geometric imperfection plus the effect of chain–chain interpenetration. As we will show, this simple approach leads to a satifactory description of the experimental data.

In practical terms, we have modeled the data using the Parratt formalism[16] rather than using the approximation, eq 1, and have assumed that except for those layers close to the substrate the system has a periodic structure.[17] To reduce computation time we have assumed one roughness, σ, at all interfaces, since we believe that the limited Q_z range assessed in the measurements does not support a more complex evaluation; note that if different interfaces in the real structure possess different roughness values ($\sigma_1 \ll \sigma_2$), then $Q_z\sigma_1 \ll 1$ holds in the Q_z range where $Q_z\sigma_2 \sim 1$, so that the impact of σ_1 on the reflectivity function can be neglected.[10]

Experimental Section

Poly(styrenesulfonate) sodium salt (PSS-h_7), M_w = 83800 ($M_w/M_n < 1.1$), was obtained from Polymer Standards Service (Mainz, Germany), and poly(allylamine) hydrochloride (PAH), M_w = 50000–65000, was obtained from Aldrich (Steinheim, Germany). Perdeuterated poly(styrenesulfonic acid) (PSS-d_7) was prepared according to the method of Vink[18] by adding 1 g of perdeuterated polystyrene, M_w = 92000 (M_w/M_n = 1.062), dissolved in 50 mL of cyclohexane dropwise to a solution of 6 g of P_2O_5 in 27 mL of D_2SO_4 at a bath temperature T = 50 °C. The solution was stirred for 80 min and allowed to stand for an additional 60 min without stirring. After the solution was cooled in an ice bath, 17 g of frozen D_2O was added. The product was isolated by cooling in a refrigerator for several days. The crude product was dissolved in 140 mL of water, exhaustively dialyzed against Milli-Q water, and freeze-dried. The yield was ~1.3 g of PSS-d_7.

Silicon substrates (~45 × 140 × 0.7 mm, Wacker, München, Germany) were cleaned using the RCA protocol[19] by immersing in 5:1:1 $H_2O/H_2O_2/NH_3$ at T = 80 °C for ~15 min,[1] followed by extensive rinsing in Milli-Q filtered water. To obtain positively charged substrate surfaces for the deposition of the first polyanion layer, the wafers were then silanized. First, they were washed for 2 min each in pure methanol (2×), 1:1 methanol/toluene (2×), and pure toluene (2×). All solvents were of p.a. grade (Merck, Darmstadt, Germany). After the last wash, the wafers were directly transferred into a 1 vol % solution of (4-aminobutyl)-dimethylmethoxysilane (ABCR, Karlsruhe, Germany) for ~16 h. Finally, the surface-modified substrates were washed again in p-toluene (2×), 1:1 methanol/toluene (2×), pure methanol (2×), and Milli-Q water (3×). Polymer films were deposited on the freshly coated wafers by immersion (30 min each) into aqueous solutions containing 3 × 10^{-3} M of the respective polyelectrolyte and 2 M NaCl, followed by dipping in Milli-Q water for 3× 1 min after each deposition step. PSS-h_7 and PAH were deposited from acidic solutions (3 × 10^{-3} M HCl). Three different film samples were investigated (cf. Figure 1): 1 layer of PSS-h_7 (sample A), [(PSS-h_7/PAH/PSS-d_7/PAH)$_8$] (Sample B), and [(PSS-h_7/PAH/PSS-h_7/PAH/PSS-d_7/PAH)$_8$] (sample C).

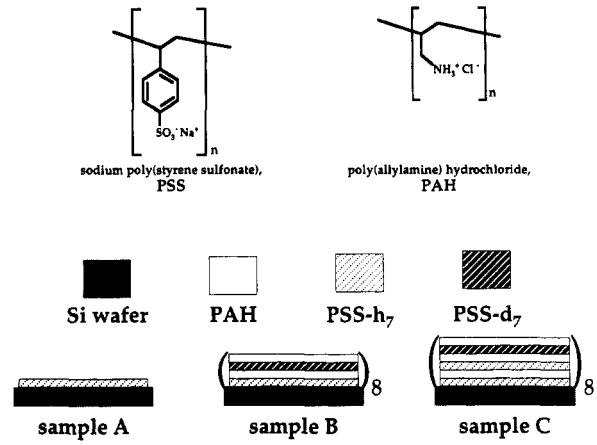

Figure 1. Chemical structures of the polymer repeat units (top) and layer motifs in the samples (bottom).

The reflectometric measurements were conducted at Risø National Laboratory. The TAS7 neutron reflectometer has a vertical scattering plane and was described earlier.[20,21] It was operated at λ = 4.64 Å. In different regimes of the momentum space different slit widths, i.e., different values of the instrumental resolution, were chosen. The X-ray reflectometer is based on a rotating-anode, Cu Kα (λ = 1.54 Å) generator and has a horizontal scattering plane with fixed-width slits. To measure over a dynamic range of 6 decades, calibrated PMMA attenuators were used at low scattering angles.

Results and Discussion

The native substrates were characterized by X-ray reflectivity measurements (data not shown). Their electron densities were found to be in accordance with published data, σ_e^{sub} = 0.705 (±0.005) e$^-$/Å^3.[11] An absorption coefficient μ_x^{Si} = 151 cm^{-1} from the literature[22] was used for the evaluation. The SiO_2 interface layer[11] was not resolved. The root-mean-square surface roughness was σ_e^{sub} = 3.9 (±0.5) Å. Figure errors (typically 0.01° of curvature across the full length of the waters, ~150 mm) were found to limit the useful resolution of the spectrometer/sample configuration to ~10^{-3} Å^{-1} with the Cu Kα wavelength. Due to the lower flux at the neutron reflectometer, which precluded taking measurements at slit widths as small as in the X-ray work, these figure errors limited the useful resolution only at low Q_z (≲0.02 Å^{-1}). At higher Q_z, a resolution on the order of ~5 × 10^{-3} Å^{-1} had to be used to obtain reasonable counting statistics.

Sample A was characterized by X-ray reflectometry only. Figure 2 shows the experimental data and the best fit to a model in which we kept the optical parameters of the Si substrate fixed. The interference effects due to the adsorbed polymer indicate a molecular layer with an electron density of ρ_e^{PSS} ~ 0.302 or ~0.406 e$^-$/Å^3 and a thickness of d_1 ~ 13.4 Å, including the aminosilane layer, which may contribute ~3–5 Å. These two alternative models are related by Babinet's theorem and produce identical reflection intensities with different phases. If the presence of counterions and residual water is neglected in the evaluation, they correspond to mass densities of ρ_m^{PSS} ~ 0.975 or ~ 1.31 g/cm^3 of the polymer. The surface roughness did not significantly differ from that of the bare substrate, indicating that the polymer film is rather continuous and exposes a smoth surface to the air.

Samples B and C were characterized by both X-ray and neutron reflectivity measurements. The experimental data for sample C, composed of 48 alternating layers of

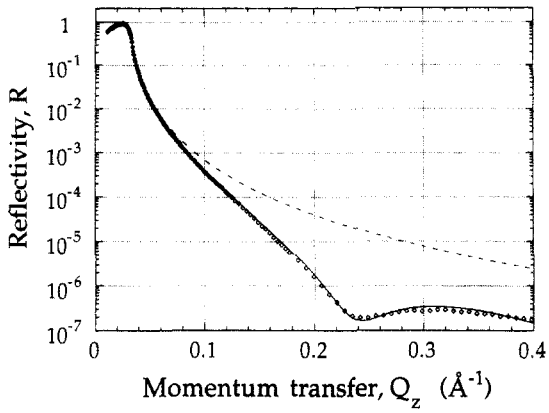

Figure 2. X-ray reflectivity of a monolayer of PSS-h_7 on silanized silicon: solid line, reflectivity calculated from the best-fit model (see text); broken line, reflectivity calculated for the bare substrate with surface roughness.

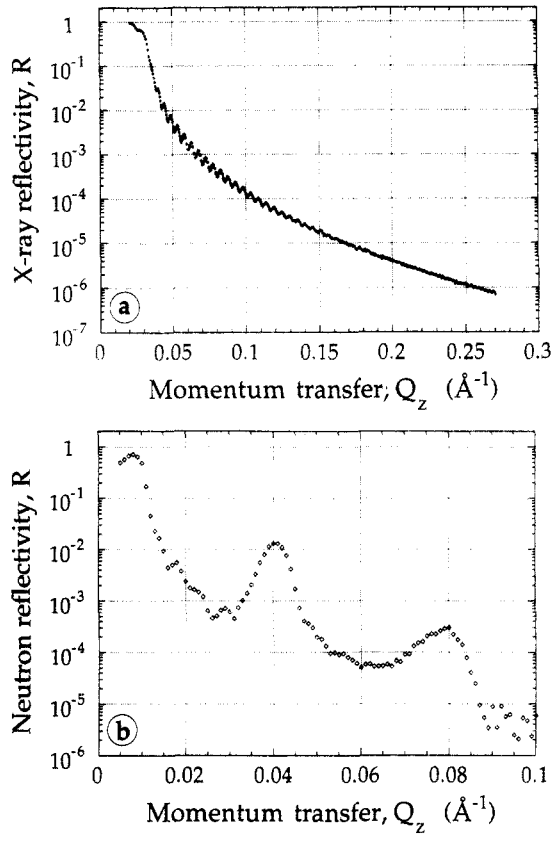

Figure 3. (a) X-ray and (b) neutron reflectivity of a 48-layer polymer film (sample C) on silicon.

charge-deposited polyanions and polycations, are shown in Figure 3.[23] The X-ray reflectivity (Figure 3a) was determined over 6 orders of magnitude. It is sensitive to only the overall structure of the thin polymer film, as shown earlier:[2] A large number, ~25, of Kiessig fringes[24] are observed in the data due to the interference of X-rays reflected from the front and the back of the polymer film, where the steepest gradients in electron density occur. The amplitude of these fringes decreases for progressively larger values of Q_z. This can be attributed to different roughness values of the substrate/film and film/air interfaces, i.e., to uneven layer thickness, either microscopically or macroscopically, on the order of 1% of the total thickness. Between the critical momentum transfer values of the polymer, $Q_c^f \sim 0.024$ Å^{-1}, and of the Si substrate, $Q_c^{Si} \sim 0.0316$ Å^{-1}, a significant reduction of the reflectivity from unity to ~0.7 is observed. It is probably due to the (small) X-ray absorption of the polymer, as indicated by

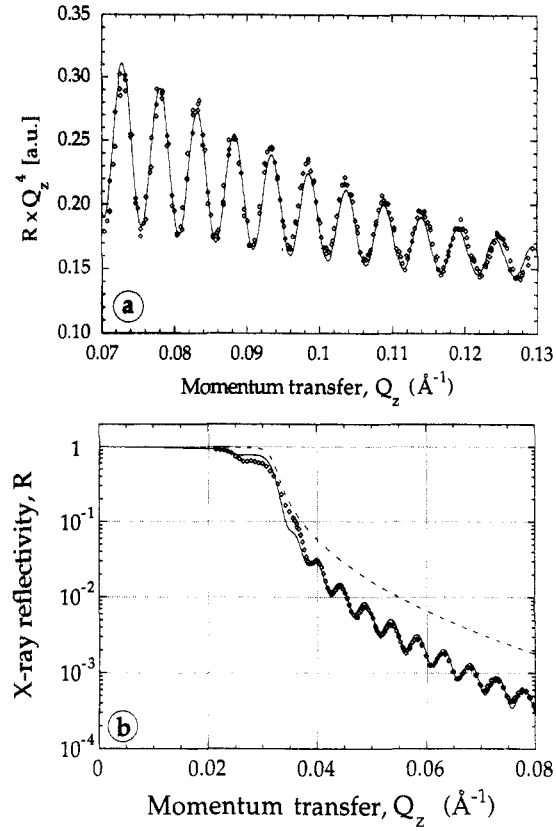

Figure 4. (a) Fit, according to eq 3, to the X-ray reflectivity data of sample C (Figure 3a) in the regime of moderately large Q_z. The Fresnel reflectivity has been approximated by $R_F \sim Q_z^4$. (b) Fit to the X-ray reflectivity data (Figure 3a) in the regime of small Q_z.

the model calculation (see Figure 4b). No Bragg reflections are observed, obviously since the electron density differences between the molecular sublayers of PSS and PAH are too small. In contrast, the neutron reflectivity (Figure 3b) shows indications of Kiessig fringes and two Bragg reflections in the data. The instrumental resolution was changed at two points during the measurement of the neutron reflectivity, as indicated by the arrows in Figure 5: $\Delta Q_z \sim 1.0 \times 10^{-3}$ Å^{-1} ($Q_z \leq 0.018$ Å^{-1}); $\Delta Q_z \sim 1.6 \times 10^{-3}$ Å^{-1} ($0.018 < Q_z \leq 0.05$ Å^{-1}); $\Delta Q_z \sim 5.2 \times 10^{-3}$ Å^{-1} (0.05 Å$^{-1} < Q_z$). The Bragg reflections result from the internal structure of the polymer film, which comprises a superlattice with deuterated PSS as every sixth layer. At a given Q_z ($>Q_c$) outside the Bragg reflections, the neutron reflectivity is a factor of ≳10 smaller than the X-ray reflectivity, in part because the absolute value of the contrast between the substrate and air is smaller by a factor of ~10 for neutrons than for X-rays; this precludes the observation of higher order Bragg peaks.

The quantitative evaluation of the data invoked different levels of sophistication: In the X-ray reflectivity data, the distance between the positions of Kiessig maxima was used to determine the total film thickness. We found that the fringe spacing was not equidistant but increased with increasing angles of incidence. This may be due to an influence of absorption of the sample (see below) in the regime of low Q_z. Consequently, as shown in Figure 4a, we have evaluated the fringe spacing at higher Q_z, between 0.07 and 0.13 Å^{-1}, and found $\Delta Q_z \sim 5.2 \times 10^{-3}$ Å^{-1}, indicative of a total film thickness of $d_{total} = 2\pi/\Delta Q_z \sim 1210$ Å.

The optical constants of the polymer film were evaluated by fitting a simple one-box model[7] to the data at low Q_z (<0.08 Å^{-1}) (cf. Figure 4b), with only one (average) surface roughness attributed to both interfaces of the polymer film. The results are compiled in Table I. The

Table I. Results of the Structural Investigation of Sample C (Six Molecular Polymer Layers of Which One Was Deuterated within the Layer Repeat Unit) from X-ray and Neutron Reflectometry

	X-ray	
d_{total}	1205 (±20) Å^2	overall film thickness
$\sigma_e^{sub} = \sigma_e^{s/f}$	3.9 (±0.5) Å	substrate/film interface roughness
$\sigma_e^{f/a}$	13–15 Å	film/air interface roughness
ρ_e^f	0.409 e$^-$/Å^3	average electron density of the film
μ_x^f	~25 cm^{-1}	average X-ray absorption cross section of the film
	Neutrons	
d_{total}	1225 (±15) Å	overall film thickness
d_{ru}	159 (±2) Å	thickness of the layer repeat unit
d_{PSS}	34 (±8) Å^2	thickness of the (deuterated) PSS layers within the repeat unit
$\sigma_n = \sigma^{int}$	19 (±1) Å	roughness of the internal interfaces within the film
ρ_n^{dt}	3.1 × 10^{-6} Å^{-2}	SD$_n$ of the deuterated PSS layers within the repeat unit
ρ_n^{pr}	0.87 × 10^{-6} Å^{-2}	SD$_n$ of the protonated interlayers within the repeat unit
	Dependent Quantities	
d_{PAH}[a]	~19 Å	thickness of PAH layers within the repeat unit
d_{first}[b]	~59 Å	thickness of the first four polymer layers plus silane layer
d_{int}[c]	~12 Å	chain/chain interdigitation between adjacent layers
n_w^{PSS}	~4	water molecules per monomeric PSS unit in the layer

[a] $d_{PAH} = d_{ru}/3 - d_{PSS}$. [b] $d_{first} = d_{total} - 22(d_{PSS} + d_{PAH})$. [c] $d_{int} = [(\sigma_n)^2 - (\sigma_e^{f/a})^2]^{1/2}$.

data were best described if a polymer layer of d_{total} = 1185 Å, ρ_e^f = 0.409 e$^-$/Å^3, and $\mu_x^f \sim 25$ cm^{-1} was assumed. In contrast to the situation with the PSS *monolayer*, where the kinematic approximation holds well and the Babinet ambiguity affects the evaluation of the structure, this approximation fails here. The full dynamic computation results in a phase shift of the Kiessig fringes by π if the film is modeled with $\rho_e^{f*} \sim 0.3$ e$^-$/Å^3 ($=\sigma_e^{sub} - \rho_e^f$). The X-ray absorption is dominated by the counterions, and the relatively large X-ray absorption cross section of the polymer film, which incorporates presumably water and counterions, can only be understood if it is assumed that, in particular, Cl$^-$ anions are included ($\mu^{PAH} \sim 45$ cm^{-1} for a 1:1 stoichiometry of Cl$^-$ and allylamine monomers in PAH films, whereas $\mu^{PAH+} \sim 4.5$ cm^{-1} if no Cl$^-$ was present; μ^{PSS} or $\mu^{PSS-} \sim 21$–22 cm^{-1}, almost independent of Na$^+$ concentration).[22] Under the assumptions that Na$^+$ cations and Cl$^-$ anions incorporate in the same stoichiometry into the polyelectrolyte multilayers and that about twice as many PAH repeat units incorporate into the molecular films than do PSS monomers, which derives its origin from the neutron results (see below), it is estimated that on average $n_{ci} \sim 0.5$–0.8 counterions incorporate per deposited monomeric unit of the respective polyelectrolytes. It can be expected that n_{ci} may be determined with sufficient accuracy by measuring precisely the absorption cross section and using heavy ions.

The roughness of the film/air interface may be estimated by using the approximation[10,11]

$$\frac{R(Q_z)}{R_F(Q_z)} \sim \left(\frac{\rho_e^{sub} - \rho_e^f}{\rho_e^{sub}}\right)^2 + \left(\frac{\rho_e^f}{\rho_e^{sub}}\right)^2 \exp(-Q_z^2\{(\sigma_e^{f/a})^2\}) + 2\frac{\rho_e^{sub} - \rho_e^f}{\rho_e^{sub}}\frac{\rho_e^f}{\rho_e^{sub}} \exp\left(-\frac{1}{2}Q_z^2\{(\sigma_e^{f/a})^2\}\right) \cos(Q_z d_{total}) \quad (3)$$

which holds in the kinematic limit if the substrate/film roughness is small, $\sigma_e^{s/f} \ll \sigma_e^{f/a}$. The decay of the amplitude of the fringe patterns was evaluated between Q_z = 0.07 and 0.13 Å^{-1} (see Figure 4a). At lower Q_z the model described the data poorly due to the nonuniform spacing of the fringes, whereas at higher Q_z data noise increased. Within these limitations, the evaluation yielded $\sigma_e^{f/a} \sim 13$ Å and d_{total} = 1220 Å. A model of the interface structure which took explicitly into account the two different surface roughnesses and was fitted to the whole data set indicated $\sigma_e^{f/a} \sim 15$ Å.[25]

In contrast to X-rays, neutrons are sensitive to the internal structure of the electrolyte film. This is clearly demonstrated by the observation of the Bragg peaks at $Q_z^{Br} \sim 0.0405$ and 0.08 Å^{-1}, indicative of a thickness of the repeat unit, [PSS-h_7/PAH/PSS-h_7/PAH/PSS-d_7/PAH], of $d_{ru} = 2\pi/Q'_z{}^{Br} \sim 160$ Å [where $Q'_z = (Q_z^2 - Q_c^2)^{1/2}$]. The observation of Bragg peaks provides the first direct evidence that the charge-deposited PSS/PAH films are composed of well-defined layers. The quantitative result implies that those molecular layers deposited close to the substrate grow to a smaller individual thickness than those further away: the overall thickness expected from d_{ru}, 8 × 159 Å, is significantly larger than the actual value d_{total} = 1205 ± 20 Å, as obtained from the X-ray experiments. Moreover, the thickness of one PSS monolayer directly deposited on the surface-modified substrate was determined as $d_1 \sim 13$ Å, smaller than $d_{ru}/6$ by a factor of ~2. On the other hand, the width of the Bragg peaks is reasonably well modeled (taking into account the instrumental resolution) if it is assumed that the 7 repeat units of the structure deposited beyond the first five layers are uniform in width (see below). It has thus to be concluded that an equilibrium growth thickness of the molecular polymer layers is reached only a few layer spacings away from the substrate.

In modeling the neutron results we have assumed unique thicknesses, d_{PSS} and d_{PAH}, for all but the four molecular layers closest to the substrate, i.e., from the first deuterated layer on. The neutron scattering length densities (SD$_n$) were assumed uniform across layers of protonated polymer; i.e., no discrimination was made between PAH and PSS-h_7. Neutron absorption cross sections of the polymers are vanishingly small and were neglected. The roughness was assumed to be equal at all interfaces. Since the roughness at the internal (see below) and the film/air interfaces is much larger than that of the substrate and dominate the latter by far, this is a reasonable approximation. The instrumental resolution was included in the fit and was found to be slightly larger around the first and smaller around the second Bragg peak than the values expected from the geometry of the instrument.[15] In Figure 5, the model reflectivity is compared with the experimental data; see Table I for quantitative results. The SD$_n$ profile used to obtain the fit is included in Figure 5 as an inset. Despite the fact that the coarse model does not reproduce all features of the experimental data very well ($\chi^2 \sim 6.5$ for the data with $Q_z > 0.018$ Å^{-1}), three prominent results emerged from the model fit:

(a) The individual thickness values of the molecular layers could be determined. The difference between the results, $d_{PSS} \sim 34$ Å and $d_{PAH} \sim 19$ Å, does not compensate for the disparity of the number of electrons on the PSS and PAH monomers, 95 vs 32. As a consequence and in connection with the approximately uniform electron density within the structured films, about 1.5× as many PAH monomers units are incorporated into the average molecular layer than PSS monomers.

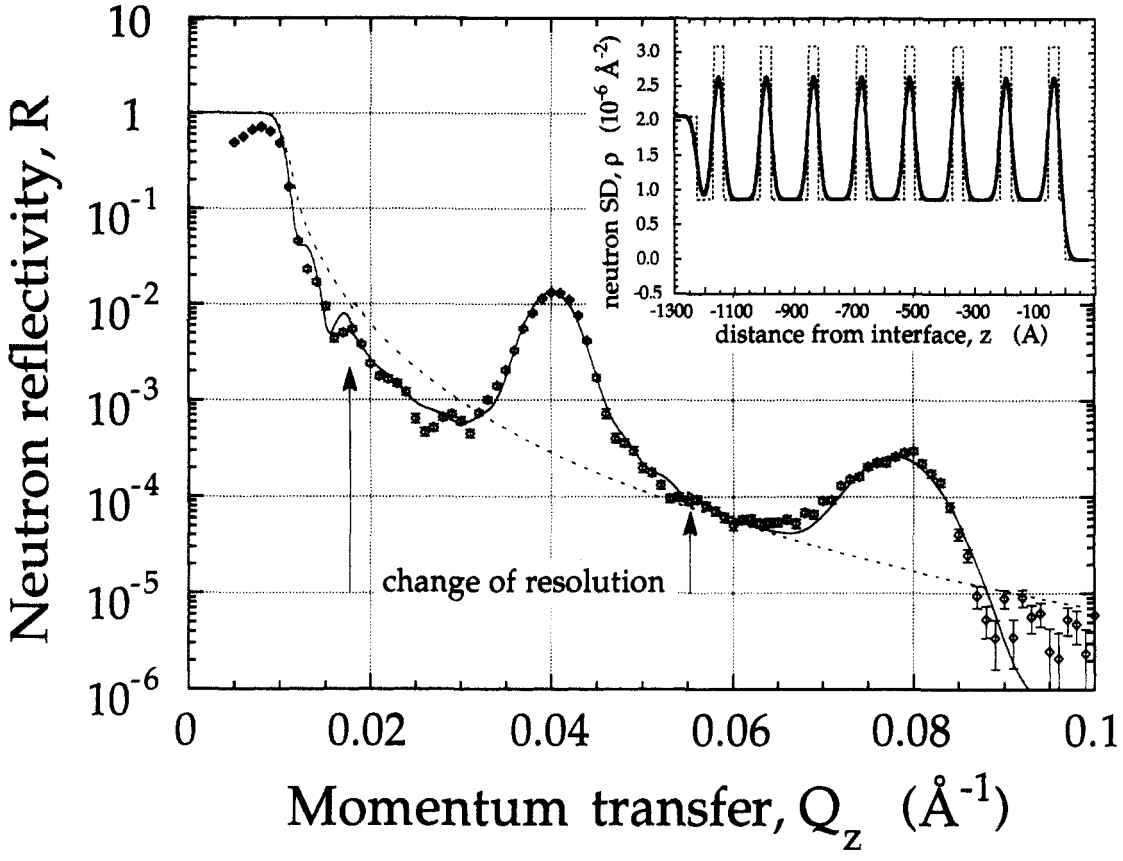

Figure 5. Fit to the neutron reflectivity data of sample C (Figure 3b). The resolution of the instrument was changed at two points, indicated by the arrows, and was included in the fit. The SD_n profile used to calculate the reflectivity (solid line) is shown in the inset. The broken line in the inset illustrates the profile as it would appear without surface roughness.

(b) The fast decay of the neutron reflectivity in Q_z in comparison to the X-ray reflectivity is not entirely due to the difference between the absolute refractive indices of the substrate for both types of radiation. Instead, the neutron data can only be quantitatively accounted for if a different surface roughness is assumed than in the interpretation of the X-ray results. In the model describing the neutron data, $\sigma_n \sim 19$ Å is distinctively larger than that of the film/air interface of the X-ray model, $\sigma_x^{f/a} \sim$ 13–15 Å. Since the major difference between neutrons and X-rays with respect to the optics of the film is that neutrons reflect from the internal interfaces whereas X-rays do not, this discrepancy has to be attributed to a larger roughness of those internal interfaces. It has thus to be postulated that chain–chain interdigitation increases the internal interface roughness.

(c) The observed magnitudes of the neutron SD's for both the deuterated and the protonated layers within the film can only be understood if it is assumed that a large portion of water is incorporated. For the PSS-d_7 layers, the water content can be precisely determined: Whereas $\rho_n \sim 5 \times 10^{-6}$ Å^{-2} would be expected from the average electron density if the layers consisted of dry polyelectrolyte plus counterions, we observe in fact $\rho_n \sim 3.1$ ($\pm$0.5) $\times 10^{-6}$ Å^{-2}. If the discrepancy is entirely due to incorporated water, then $n_w^{PSS} \sim 4$ ($\pm$1.5) water molecules are incorporated per PSS-d_7 repeat unit.

The detailed picture which evolves from the results presented above may be summarized as follows: PSS/PAH polyelectrolyte films deposit as well-defined molecular layers. Those layers deposited close to the substrate show a much smaller film thickness than those further away, where the layer thickness attains an equilibrium value. For PSS deposited from 2 M NaCl solutions, the first layer has a thickness of ~13 Å, whereas the equilibrium thickness is ~34 Å. For PAH deposited from 2 M NaCl we have not measured the thickness of the first layer, but it may be inferred from the small distance of the first deuterated layer to the substrate that this thickness is on the order of 10 Å, as in the PSS case. The equilibrium thickness of PAH layers is ~19 Å under these conditions.

To describe the neutron reflectivity from sample C, we have assumed that (only) the first four protonated layers differ in thickness from all other layers. This led to an unrealistically small result for the combined thickness of these inner layers. It has to be concluded that the equilibrium thickness is reached only for higher layer numbers and implies that the first deuterated layer does not exactly match the lattice position within the superlattice in the film. We found that the apparent instrumental resolution, as obtained from the fit, was coarser than the value calculated from the geometry of the instrument. This suggests that the Bragg peak was inherently broader than expected for an array of 7 repeat units within the superlattice, which would be consistent with the assumption that the equilibrium layer thickness is reached only beyond the fourth layer deposited.

Three different interface roughnesses have to be distinguished in the system: the substrate/film interface is smooth, $\sigma^{s/f} \sim 4$ Å; the film/air interface has a much higher roughness but is still almost molecularly smooth, $\sigma^{f/a} \sim$ 13–15 Å; the internal interfaces between the individual layers show the largest roughness, $\sigma^{int} \sim 19$ Å. This may be attributed to chain–chain interdigitation between molecules from adjacent layers. If one assumes that the contribution to the roughness, which is due to interdigitation, occurs at a similar in-plane length scale but is not correlated with the natural surface roughness of the polymer film, as it appears at the film/air interface, then

the length scale of interdigitation is $d_{int} = [(\sigma^{int})^2 - (\sigma^{f/a})^2]^{1/2}$ ~11–13 Å.

The scattering length densities in the system (average electron density of the film and neutron SD_n of the individual layers within the superlattice) have been determined and the X-ray absorption cross section of the film has been estimated. These results can be used to infer the composition of the molecular films in terms of its constituents: polyelectrolyte, water, and counterions. It has to be stressed, however, that this assessment occurs in a system with strongly interdependent parameters and that not all of the relevant quantities have been determined precisely enough to date. Furthermore, one has to keep in mind that the results may be model-dependent.

The partial volumes of the polyelectrolyte repeat units are rather insensitive to variation of the other quantities: We infer $V_{PSS} \sim 240$–250 Å^3 and $V_{PAH} \sim 75$–80 Å^3 under the assumption of identical mass densities, which evaluates to $\rho_m \sim 1.24$ g/cm^3. The content of counterions determines critically the X-ray absorption cross section of the film; however, the absorption has not been measured with sufficiently high precision. We estimate that ~0.5–0.8 anions or cations incorporate into the film with each repeat unit of the polyelectrolyte. X-ray reflectivity measurements on films deposited from solutions containing heavy ions are expected to enable a precise determination of this number. The water content can be precisely determined in the (deuterated) PSS layers, but less so in PAH layers. About 4 water molecules are associated with 1 PSS monomer, equivalent to ~27 wt %. On this basis it is estimated that the PSS layers are composed of ~66 wt % polymer, ~27 wt % H_2O, and ~7 wt % Na^+ ions. The composition of the protonated segments of the film cannot be determined with precision owing to the smaller SD_n in these regions. The data indicate that more Cl^- counterions are present in the PAH layers than Na^+ in PSS (by weight), at the expense of water, whereas the content of (dry) polymer is comparable to that of PSS in the deuterated molecular layers.

With X-ray and neutron reflectometry we have also investigated sample B, which was prepared under the same environmental conditions as sample C but incorporated only 4 molecular polymer layers in its repeat unit (data not shown). Kiessig fringes between $Q_z \sim 0.05$ and 0.15 Å^{-1} indicated a total film thickness of ~780 ± 10 Å. The thickness of the repeat unit was ~105 Å, as determined from a single Bragg reflection in the neutron reflectivity measurement at $Q_z \sim 0.06$ Å^{-1}.

Conclusions

The internal structure of layer-by-layer deposited polyelectrolyte film has been assessed. For the first time it has been shown that in such systems the material is indeed deposited in individual molecular layers and that the length scale of chain–chain interdigitation is less than the layer thickness, ~12 vs 20–30 Å under the preparation conditions employed here. It has been observed that the layers deposit with a small thickness close to the substrate and reach an equilibrium thickness, presumably only after the fourth deposited layer. Inorganic counterions codeposit from the aqueous solution and are responsible for the absorption phenomena observed in the X-ray experiments. Besides the counterions, water is present in sizable amounts within the films if they are handled in ambient environment. This study opens the field for systematic investigations of the experimental parameters controlling the microstructure of such polymer films and, thus, of correlating their structure to their macroscopic properties.

Acknowledgment. We are indebted to H. Möhwald for stimulating discussions and to D. Vaknin for valuable advice on the measurements. Silicon substrates and deuterated polystyrene were kind gifts from Wacker GmbH, Burghausen, and T. Wagner, Max-Planck-Institut für Polymerforschung, respectively. Financial support came from the Commission of the European Community through the Large Installation Plan, the Bundesministerium für Forschung and Technologie (Contract No. 05 453 FA 19), and the Deutsche Forschungsgemeinschaft (Contract No. De422/5-1). Partial support for P.S.P. came from the U.S. National Science Foundation, Grant NSF-DMR-91-13782.

References and Notes

(1) Decher, G.; Hong, J.-D.; Schmitt, J. *Thin Solid Films* **1992**, *210/211*, 831.
(2) Decher, G.; Schmitt, J. *Prog. Colloid Polym. Sci.* **1992**, *89*, 160.
(3) Lvov, Y.; Decher, G.; Möhwald, H. *Langmuir* **1993**, *9*, 481.
(4) Decher, G.; Lvov, Y.; Schmitt, J. *Thin Solid Films*, in press.
(5) Zhou, X.-L.; Chen, S.-H. *Phys. Rev. E* **1993**, *47*, 3174.
(6) Miyano, K.; Asano, K.; Shimomura, M. *Langmuir* **1991**, *7*, 444.
(7) Als-Nielsen, J.; Kjaer, K. In *Phase Transitions in Soft Condensed Matter*; Riste, T., Sherrington, D., Eds.; Plenum Press: New York, 1989; p 113.
(8) Lösche, M. in *Synthetic Microstructures in Biological Research*; Schnur, J. M.; Peckarar, M., Eds.; Plenum Press: New York, 1992; p 91.
(9) Pershan, P. S. *Faraday Discuss. Chem. Soc.* **1990**, *89*, 231.
(10) Russell, T. P. *Mater. Sci. Rep.* **1990**, *5*, 171.
(11) Tidswell, I. M.; Ocko, B. M.; Pershan, P. S.; Wasserman, S. R.; Whitesides, G. M.; Axe, J. D. *Phys. Rev. B* **1990**, *41*, 1111.
(12) Russell, T. P.; Karim, A.; Mansour, A.; Felcher, G. P. *Macromolecules* **1988**, *21*, 1890.
(13) Anastasiadis, S. H.; Russell, T. P. *J. Chem. Phys.* **1990**, *92*, 5677.
(14) Als-Nielsen, J.; Christensen, F.; Pershan, P. S. *Phys. Rev. Lett.* **1982**, *48*, 1107.
(15) Braslau, A.; Pershan, P. S.; Swislow, G.; Ocko, B. M.; Als-Nielsen, J. *Phys. Rev. A* **1988**, *38*, 2457.
(16) Parratt, L. G. *Phys. Rev.* **1954**, *95*, 359.
(17) Surface roughness was accounted for by multiplication with the Debye–Waller factor, $\exp\{-(Q_z\sigma)^2\}$.
(18) Vink, H. *Makromol. Chem.* **1980**, *182*, 279.
(19) Kern, W. *Semiconductor Int.* **1984**, *94*.
(20) Vaknin, D.; Kjaer, K.; Als-Nielsen, J.; Lösche, M. *Makromol. Chem., Macromol. Symp.* **1991**, *46*, 383.
(21) Vaknin, D.; Kjaer, K.; Als-Nielsen, J.; Lösche, M. *Biophys. J.* **1991**, *59*, 1325.
(22) Burr, A. F. *Handbook of Chemistry and Physics*, 57th ed.; CRC Press: Cleveland, 1976; p E139.
(23) Data presented at the 205th National Meeting of the American Chemical Society, Denver, 1993.
(24) Kiessig, H. *Ann. Phys.* **1931**, *10*, 769.
(25) We thank A. Leuthe (Mainz) for the use of his modeling routine.